NUMERICAL-THEORETICAL EVALUATION OF THE DITCHING OF A HULL WITH DIHEDRAL ANGLES BETWEEN -5 AND 20 DEGREES

Guagliardo D.[1,a], Cestino E.[1,b], Virdis A.[1], Alfero A.[1] & Sapienza V.[1]

[1]Politecnico di Torino (DIMEAS), Corso Duca degli Abruzzi, 24 10129 Torino, Italy
[a]teams55.polito@gmail.com
[b]enrico.cestino@polito.it

Abstract

The purpose of this paper is to present a detailed analysis of the impact of the hull of the S55 seaplane on a still water surface. The hull features a unique geometry, including areas with zero and negative dihedral angles, which can result in the formation of air pockets phenomena not addressed in existing literature theories.
The objective is to expand knowledge compared to the research previously conducted, where a wedge at different dihedral angles and a simplified three-dimensional geometry impacting the water under various initial conditions were respectively studied. This study will involve two comparisons: to verify the effects of the three-dimensionality of a hull impacting with only vertical velocity, the obtained results will be compared with the respective two-dimensional cases modeled through wedges; and to measure the pressures that develop on the hull upon impact with the water, also in the presence of a horizontal velocity component.
Special attention will be given to pressure in the case of zero or negative dihedral angle, for which analytical theories present unrealistic values, to assess the effect of trapped air. Numerical analyses will be conducted using the ANSYS LS-DYNA solver, modeling wedges and the hull with shell elements and employing steel as the material. Water will be modeled using the SPH method, with properties referring to standard conditions. Air will also be introduced through the same method, and results will be compared in its absence as well. Where applicable, the obtained data will be compared with the theoretical results derived from the studies on rigid wedges by von Karman and Wagner. This analysis aims to contribute to a better understanding of these phenomena, especially in a three-dimensional case.

Keywords: Fluid-Structure interaction, 3D impact on water, small dihedral angle impact, SPH

1. Introduction

Team S55 was founded in February 2017 by a group of students from the DIMEAS department at the Politecnico di Torino. The goal is to create a flying model of the historic SIAI-Marchetti S55X seaplane at a 1:8 scale (Figure 1), using the latest engineering techniques [1].

Figure 1 – TeamS55 seaplane model

This study, conducted by the Fluid-Structure Interaction division, focuses on simulating the impact of the hull on the water, building upon the research conducted in previous studies [2, 3, 4]. As can be observed from Figure 2 and Figure 3, the hull in question has a particularly interesting shape, with dihedral angles ranging from -5 to 30 degrees. The focus will be predominantly on the part of the hull that impacts first, namely that between 50% and 90% of the length, where the dihedral angle is at most 20 degrees. LS-DYNA solver is used for this purpose, and typically, the hull's shape is simplified to that of a 2D wedge for calculations, a common method in this field of studies.

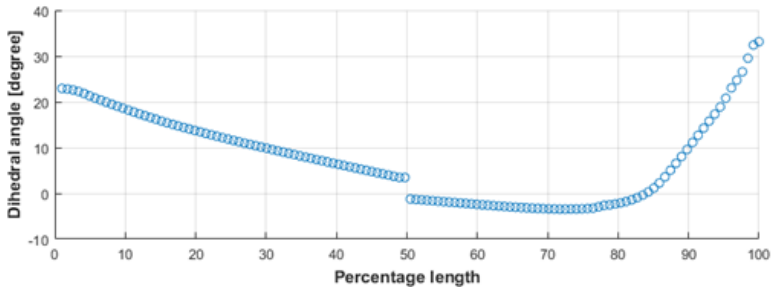

Figure 2 – Dihedral angles along the length of the hull

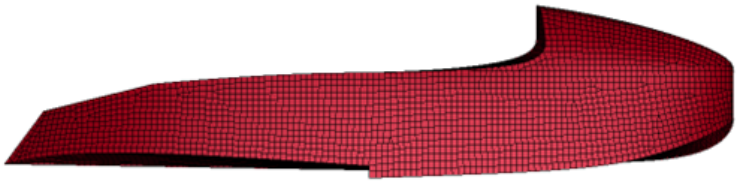

Figure 3 – Hull of the S55

The dynamic interactions related to the impact of structures with water constitute a broad and complex problem that has been studied since 1929 by von Karman [5]. Subsequently, various scholars have engaged with the issue, among them, we mention Wagner [6], whose studies date back a few years later, up to more recent theories such as that of Okada-Sumi [7]. From the early studies of von Karman, as he reports, the improbability of results for small dihedral angles and flat bodies has been discovered. Subsequently, more accurate theories were developed, aiming to consider all the various phenomena that can occur during the impact phases of a structure in water, such as air cushioning, cavitation, suction, and ventilation. The presence of these phenomena and the difficulties arising from their analyses are therefore transferred to computational software, which takes on the task of numerically simulating the multi-physics interaction between the fluid and the structure. Studies on the interaction of water with seaplanes, re-entry modules and commercial aircraft represent just a few examples of the fields of application of Fluid-Structure Interaction (FSI) studies. In fact, structures designed to absorb energy during an impact on hard surfaces don't work properly in a ditching event [8], this results in a uniformly distributed pressure on the bottom of the structures, which can lead to skin fracture (Figure 4). It is therefore interesting to analyze the behaviour of impacting bodies in order to understand the conditions that would generate excessive accelerations, endangering the safety of the occupants and the integrity of the payload.

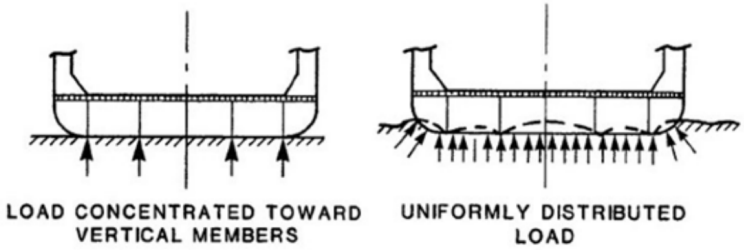

Figure 4 – Difference in load transmission during a hard impact (left) and a water impact (right) [8]

This study will show the comparison of several models, starting with an extremely simplified model and then moving on to the most complete model. The first model is a simple wedge shape representing the local section of the hull. Since the hydroplane hull is inhomogeneous in its dihedral angle, the study will include a variation in the angle of the latter. Next, the wedge will be compared with analyses performed introducing the air and then arrive at the complete model of the hull in its entirety.

2. 2D model

The model in question represents a local section of the hull in the form of a wedge. For simplicity, as already studied [4], a whole wedge is not taken but its half has no substantial difference between the two results in terms of quality of results. The material chosen for these analyses is elastic in order to consider pressure attenuation due to the deformation of the wall itself.
The wedge mechanical properties are those of a generic steel alloy, with Young's modulus of 190 GPa and a Poisson ratio equal to 0.3, simulated through LS-DYNA with two keywords. MAT_001-ELASTIC was used for the lower part, i.e., the part subject to the study, while for the upper part, in addition to having a less computational cost, it was given the material formulation MAT_020-RIGID. The dimensions, Figure 5, is 120 mm along x and 30 mm in y, while the height varies depending on the dihedral angle, and ranges from a minimum of 20 mm in the case of 0 degrees to a maximum of about 64 mm in the case of 20 degrees. The thickness of the entire skins 2 mm in all the cases studied.

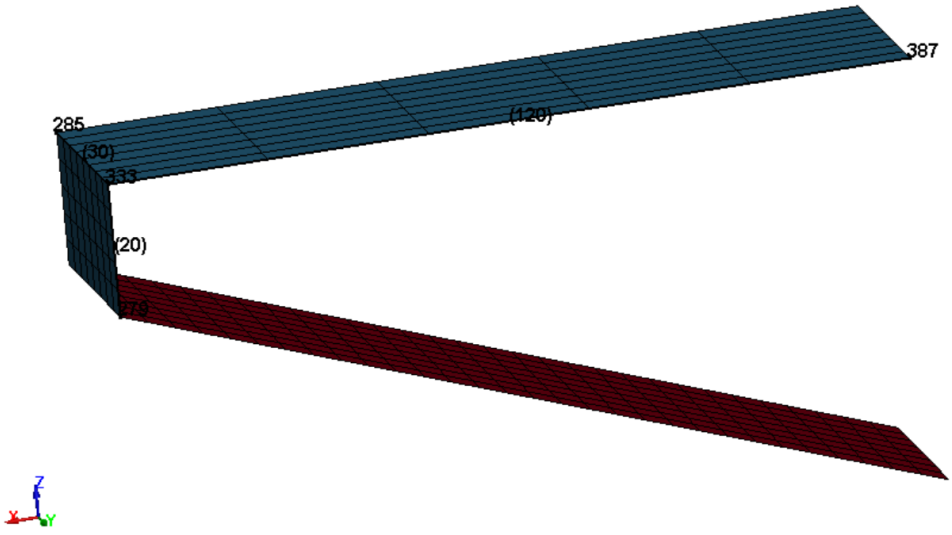

Figure 5 – Wedge dimensions

To compare the wedge with the complete hull, the four dihedral angles located in the area of initial water impact were considered, each at different initial sinking speeds. The variables investigated are reported in the following table.

α [deg]	-5	0	10	20
v [m/s]	1	3	5	

Table 1 – List of dihedral angles

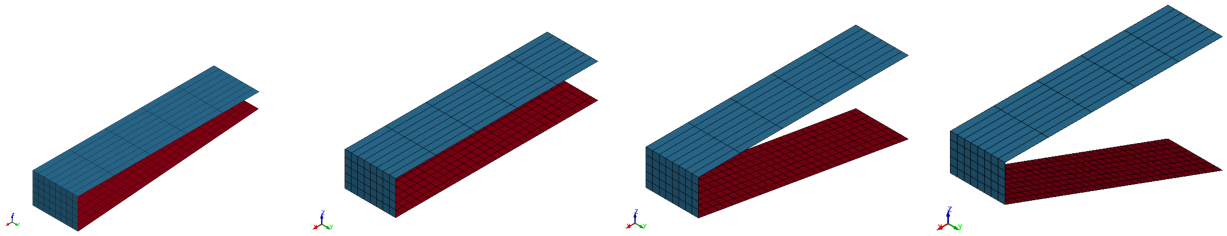

Figure 6 – Wedges with different dihedral angles

The water is modeled using the Smoothed-Particle Hydrodynamics (SPH) method, which simulates the fluid with a Lagrangian approach. These spherical elements, numbering 120,000, are placed in a tank with dimensions of 500 mm along the x-axis, 30 mm along the y-axis, and 300 mm along the z-axis. The following considerations about the wall are shown in Figure 7, where the model used for the wedge is presented. To avoid edge effects in the y direction and to account for the symmetric behavior within the unsimulated half wedge, three walls with the keyword BOUNDARY_SPH_SYMMETRY_PLANE were placed: the right wall (green), the wall perpendicular to the y-axis (blue), and the one left blank to show the model. Additionally, a rigid wall is located at the bottom using the keyword RIGIDWALL_PLANAR. Finally, another wall (gray) with the keyword BOUNDARY_SPH_NON_REFLECTING is placed at the farthest part from the wedge, simulating downstream infinity.

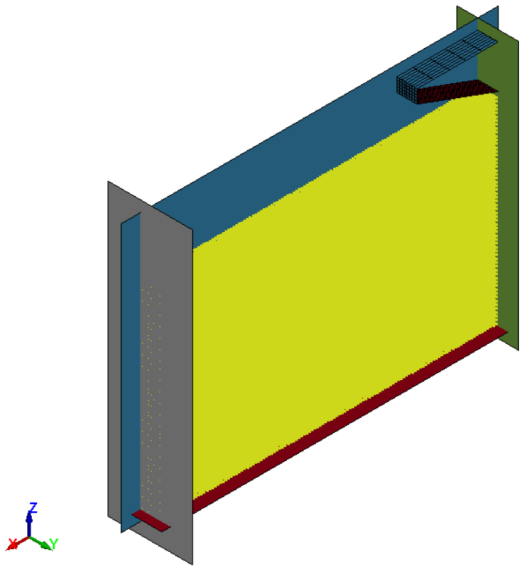

Figure 7 – Wedge model

Lastly, six pressure sensors were considered, located as shown in Figure 8. The chosen order places sensor P1 closest to the keel, 6 mm far from the edge along the x-axis, while sensor P6 is at the highest point, located 100 mm far from the first one. The sensors in the middle are equally spaced between those at the ends, and therefore are 20 mm apart from each other.

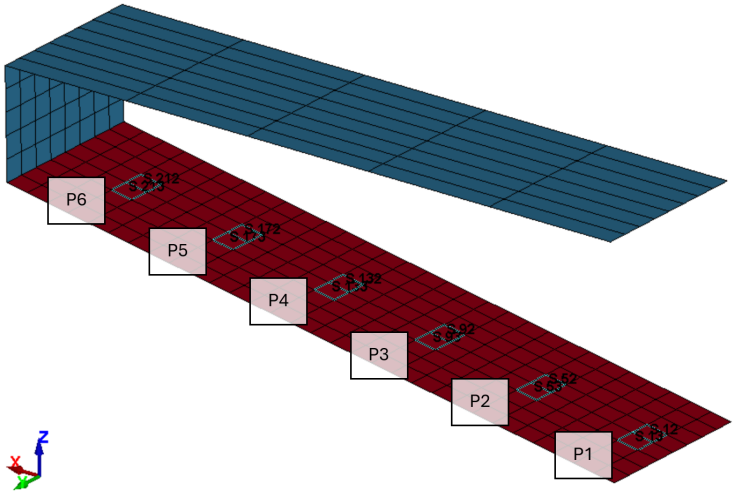

Figure 8 – Sensors position on the wedge

2.1 Comparison with analytical theories

In the first stages of the analyses, it's important to compare the results obtained with the software and the ones predicted by analytical theories. Two notable theories, which remain influential today and with the former still recognized by EASA regulations, were formulated by von Karman [5] and Wagner [6]. In both cases, we can find a prediction of the maximum pressure during a ditching event as a function of the density of water ρ, the vertical velocity v_0 of the body, and the dihedral angle α of the wedge. In the case of Von Karman's formula the maximum pressure is given by:

$$P_{VKmax} = \frac{\rho v_0^2}{2} \pi cot\alpha \tag{1}$$

On the other hand, Wagner's theory predicts a different value equal to:

$$P_{W_{max}} = \frac{\rho v_0^2}{2} \left[1 + \frac{\pi^2}{4\tan^2 \alpha} \right] \tag{2}$$

The two theories were written considering a rigid wedge, so the expected results are lower than those predicted due to the deformation of the skin. First of all, we can have three types of pressure distribution based on the dihedral angle considered during the free fall of a wedge into water. All the following analysis were performed using a wedge impacting the water with an initial vertical velocity of 3 m/s.

i. Positive dihedral angle: the pressure distribution exhibits the behavior observed in previous studies [3, 4]. As illustrated in Figure 9, it can be observed that the maximum pressure occurs at the first sensor and corresponds to the earliest time point. As the wedge continues to drop, the flow also affects the subsequent sensors, which register lower pressure peaks.

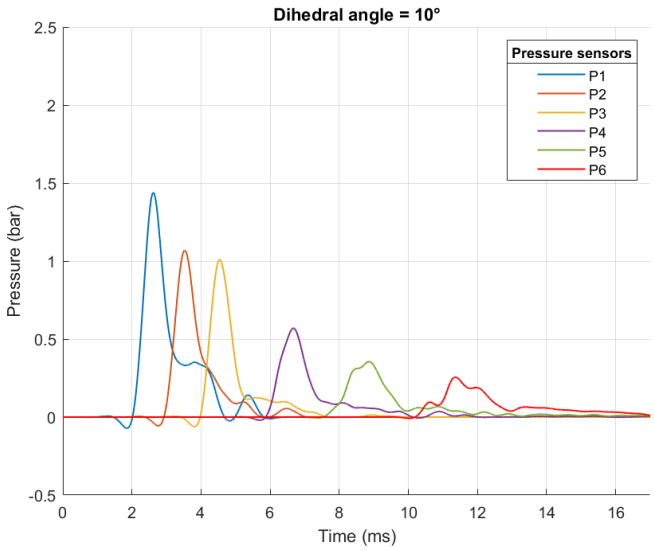

Figure 9 – Pressure in case of dihedral angle = 10°

ii. Zero dihedral angle: in this case, water impacts the entire surface of the wedge simultaneously, as evidenced by all sensors registering peaks at the same time. The three sensors closest to the keel record lower pressure due to wall deformation, whereas the three sensors at the opposite end exhibit higher pressures being closer to the rigid portion limiting deformation. This phenomenon is further highlighted by a secondary peak observed on the first three sensors, indicating a re-impact with the fluid after initially displacing it.

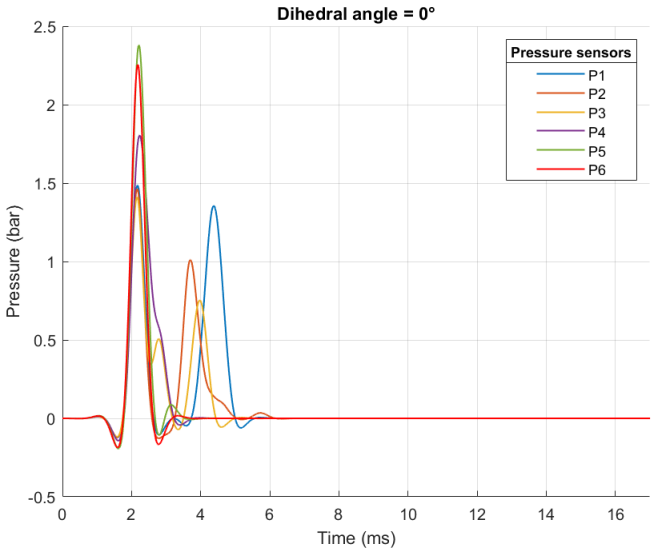

Figure 10 – Pressure in case of dihedral angle = 0°

iii. Negative dihedral angle: the observed pressure pattern demonstrates a parallel trend to that of the initial scenario concerning the position of maximum pressure relative to the specified sensor. However, it diverges concerning the sequence in which this peak is attained compared to the remaining sensors. Specifically, the maximum pressure is detected at sensor 1 subsequent to all other sensors reaching and exceeding their peak values. The timing of pressure registration differs from the two preceding cases due to the initial height from which the wedge was

released. However, this does not affect the overall trend of the analysis.

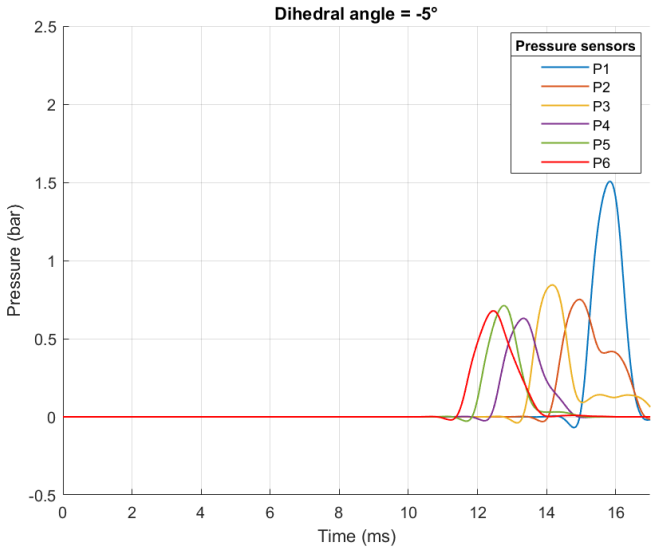

Figure 11 – Pressure in case of dihedral angle = $-5°$

From the data, it can be observed that the highest pressure is obtained, at the same speed, when the dihedral angle is zero. Additionally, the pressure trend for a dihedral angle of 20° is similar to that reported for the 10° analysis, but with lower pressures. Figure 12 presents the maximum recorded pressures, comparing these values with those predicted by von Karman and Wagner's theories.

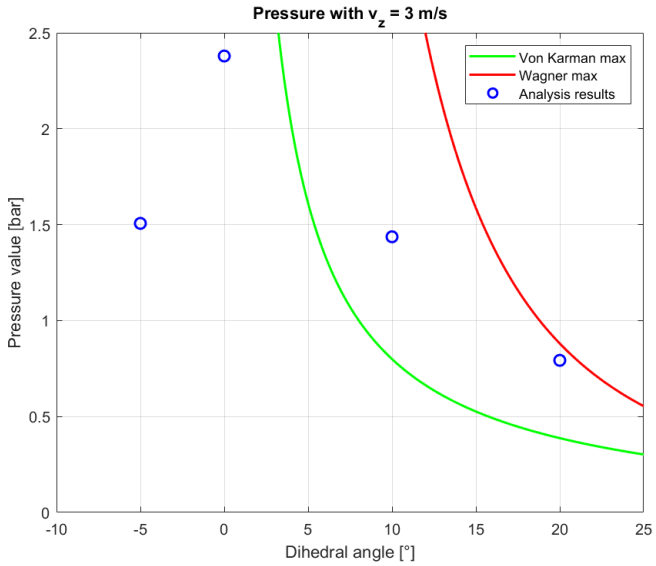

Figure 12 – Comparison of pressures varying dihedral angle

Dihedral angle [deg]	Pressure peak [bar]
-5	1.506
0	2.379
10	1.436
20	0.792

Table 2 – Pressure as a function of dihedral angles

In Figure 12, it is observed that in the case of analysis at 3 m/s and positive dihedral angles, the maximum pressure value falls between the curves of the two analytical theories. However, in the case of a zero dihedral angle, these theories predict an infinite value, which is not physically realistic. The maximum pressure measured is 2.379 bar, as previously reported in Figure 10. Finally, for the considered dihedral angle, the recorded pressure is lower than the maximum value, at 1.506 bar.
In Figures 13, 14, and 15, the calculated pressure values are compared with the formulations from the literature, considering the dihedral angle as constant while varying the velocity. As previously mentioned, it is not possible to consider the estimated pressure for the case of a zero-degree angle, as it is theoretically infinite.

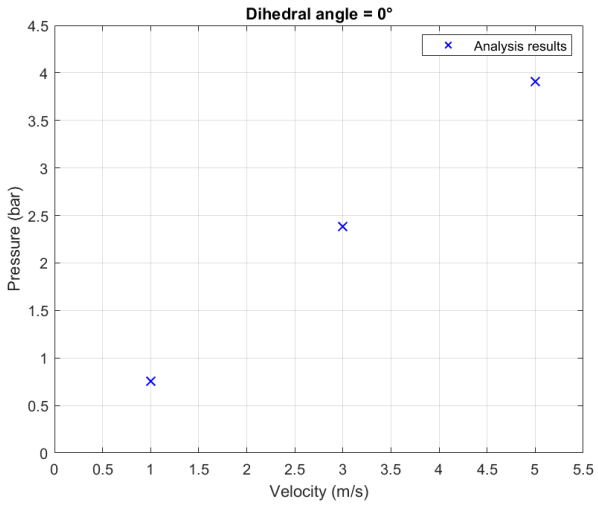

Figure 13 – Comparison of pressures varying vertical velocity, $\alpha = 0^\circ$

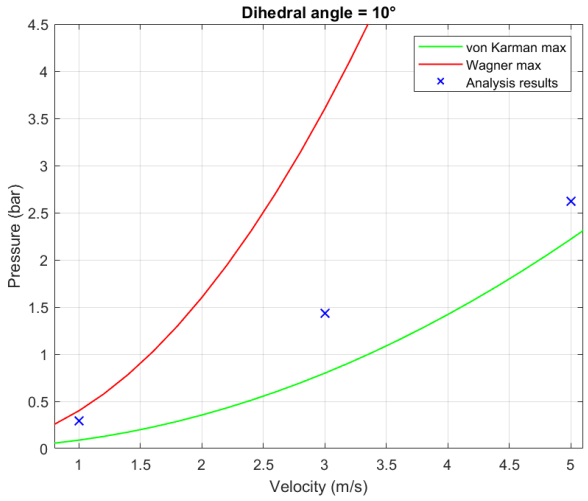

Figure 14 – Comparison of pressures varying vertical velocity, $\alpha = 10^\circ$

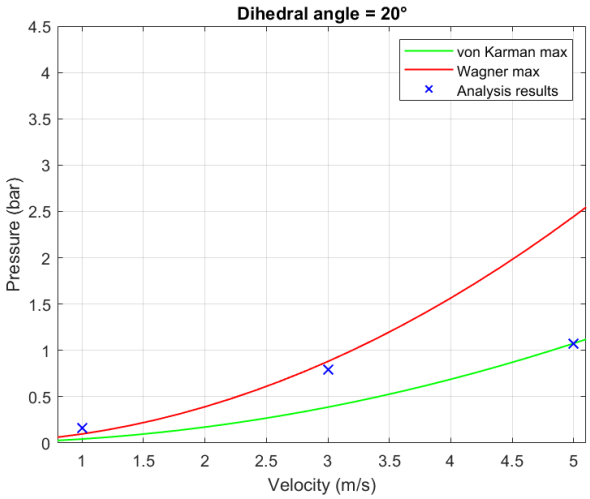

Figure 15 – Comparison of pressures varying vertical velocity, $\alpha = 20^{\circ}$

What can be observed from the graphs above is that the material's elasticity becomes significant at higher speeds, where the deformations are non-negligible. Furthermore, in the case where the dihedral angle is zero, the pressure's dependence on speed appears to increase linearly with a coefficient of 0.787. Therefore, the pressure can be expressed as:

$$P_{0^{\circ}} = 0.787 * V \tag{3}$$

2.2 Air introduction

To have a more accurate model closer to reality, air was also considered to be added, again using the SPH method with the keyword *MAT_ELASTIC_FLUID-ELASTIC. Figure 16 depicts the air, represented in blue, in direct contact with the water elements, completely enveloping the body. The interaction between air and fluid was facilitated using the *DEFINE_SPH_TO_SPH_COUPLING keyword. Additionally, a *BOUNDARY_SPH_NON_REFLECTING wall was implemented at the top of the box to simulate the presence of an overlying air column. The wedge was raised 30 mm compared to the airless scenario to prolong its interaction with the air elements, allowing for a more in-depth examination of their interaction.

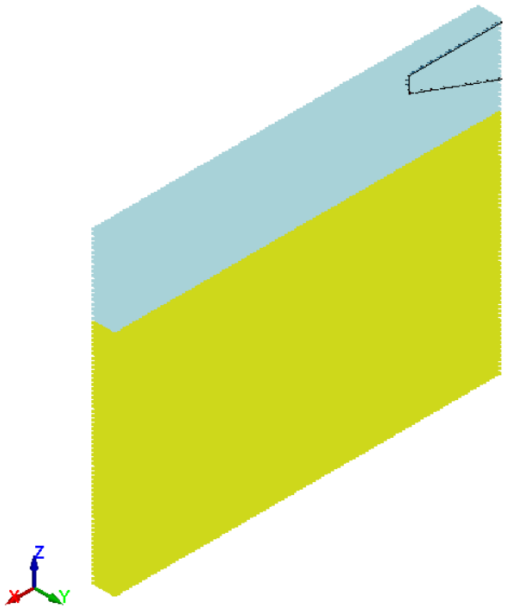

Figure 16 – Wedge model with air

The inclusion of air is often neglected due to the high computational cost of such analyses; however, it significantly affects small dihedral angles. Analyses were conducted for wedges with an initial speed of 3 m/s and dihedral angles of -5°, 0°, 10°, and 20°. The results (Figure 17) indicate that air generally exerts a beneficial effect, particularly evident in the cases of zero and negative angles. For the positive angles considered, the results closely align with von Karman's analytical theory.

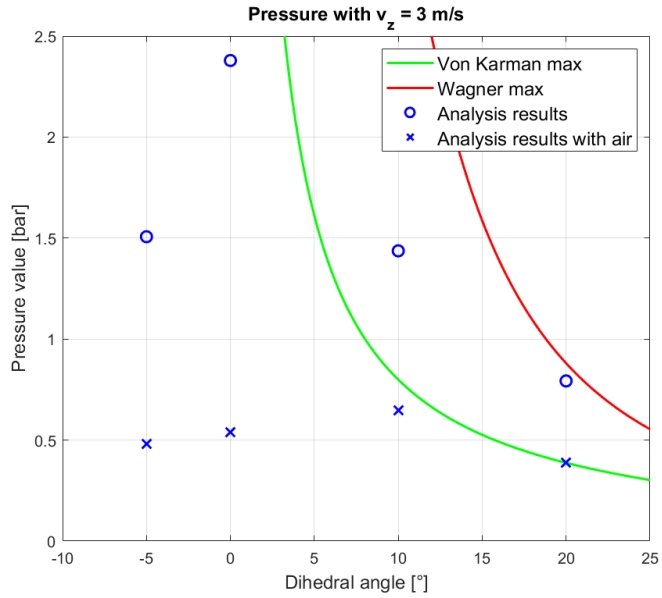

Figure 17 – Comparison of pressures varying dihedral angles

Additionally, the simulations reveal that for zero and negative dihedral angles, an air pocket forms between the water and the wedge. This phenomenon is not observed for positive dihedral angles, where the air escapes laterally. It is noteworthy that air does not affect the impact velocity until the wedge contacts the water or the air-water mixture, as shown in Figure 18 in a scenario wherein the wedge, characterized by a dihedral angle of 10°, has an initial velocity of 3 m/s. Moreover, the inclusion of air results in lower peak pressures and a relatively smoother pressure distribution.

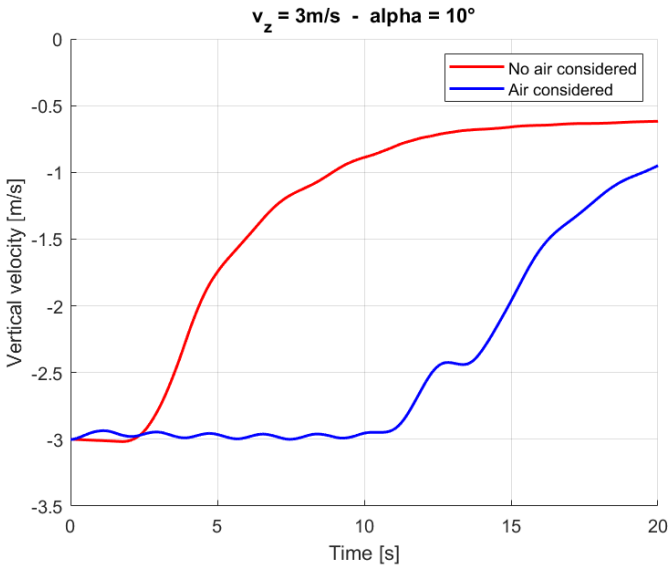

Figure 18 – Velocity vs. Time graph for the analysis at 3 m/s with a dihedral angle of 10°

3. 3D model

The hull design is based on the original geometry of the Savoia-Marchetti S55 seaplane hull, scaled down to 1:8 from the original size. The dimensions of the scaled model under study are as follows:

- 1236.1 mm in the longitudinal direction;
- 243.2 mm at the point of maximum width;
- 288.9 mm between the points of maximum and minimum height.

To minimize computational expense, only half of the model was analyzed using a symmetry boundary condition, as this does not substantially affect the accuracy of the results. Additionally, the model was divided into two distinct *PART, allowing the application of two different material formulations, as illustrated in Figure 19. This approach permitted deformations only in the area of interest, further reducing computational cost where there is no contact with the fluid. The two parts were defined as follows:

- The upper part (red) has modeled with the keyword *MAT_RIGID, assumed to be infinitely rigid. This part will not come into contact with the fluid.
- The lower part (blue) has modeled with the keyword *MAT_ELASTIC. This part is of primary interest as it will come into contact with the fluid.

Both parts, each 2 mm thick, are composed of a generic steel alloy with an elastic modulus of 190 GPa and a Poisson's ratio of 0.3. The total mass of the entire hull amounts to 6.412 kg. Additionally, some boundary conditions have been applied: specifically, rotations around the Y-axis and Z-axis (roll and yaw) have been constrained for the upper rigid part, and movements have been restricted along the X-axis.

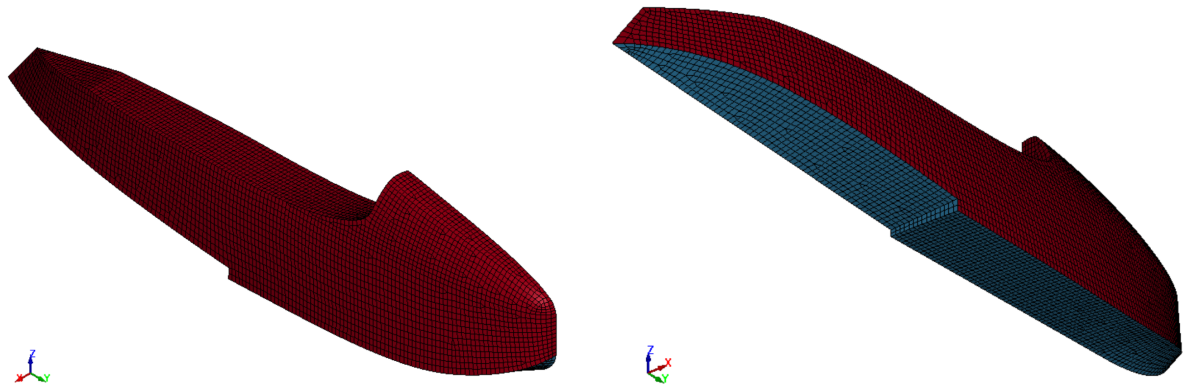

Figure 19 – S55's hull, isometric view and from below

Regarding the water tank created, it has dimensions of 500 mm in the x and z directions and 1500 mm in the y direction. The walls, depicted in Figure 20, are defined as follows: one *BOUNDARY_SPH_SYMMETRY_PLANE wall (the blue one), one *BOUNDARY_SPH_NO_REFLECTING wall to prevent wave reflection (hidden to allow model visualization), and three *RIGIDWALL_PLANAR walls represented in green, red, and gray.

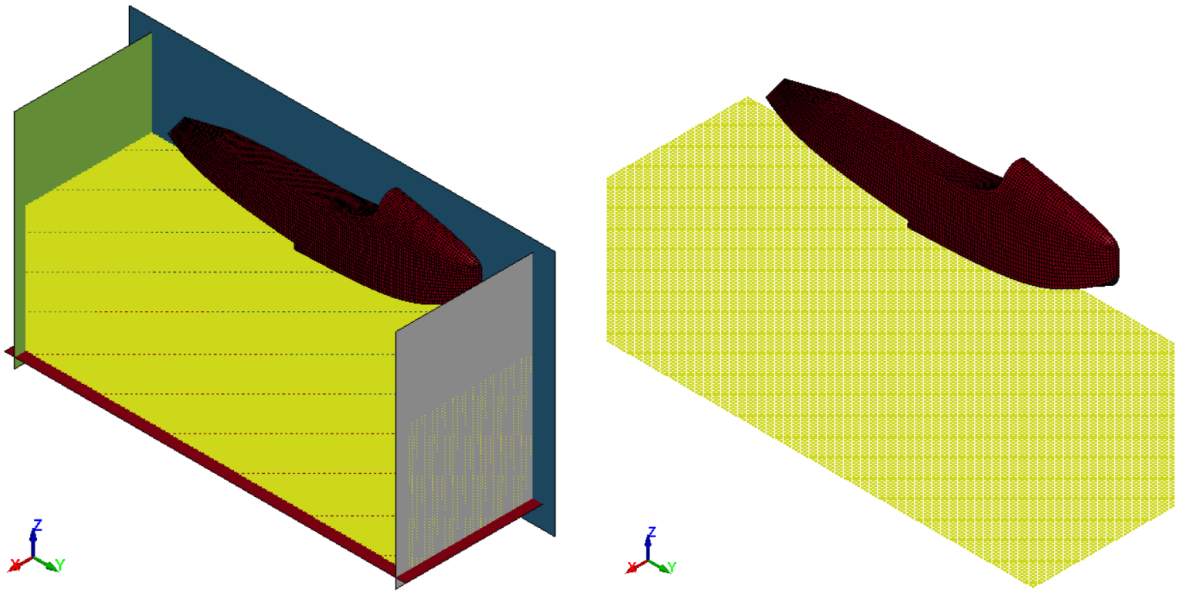

Figure 20 – Full model

Several analyses have been conducted on the hull model, studying the impact on water at different speeds. Pressure sensors have been selected in the area ranging from approximately 50% to 90%, Figure 21, thus studying the pressure variation with changes in the dihedral angle. Subsequently, the analyses will be compared with those performed on the wedge at the same speed, to study the introduction of effects due to the three-dimensionality of the model.

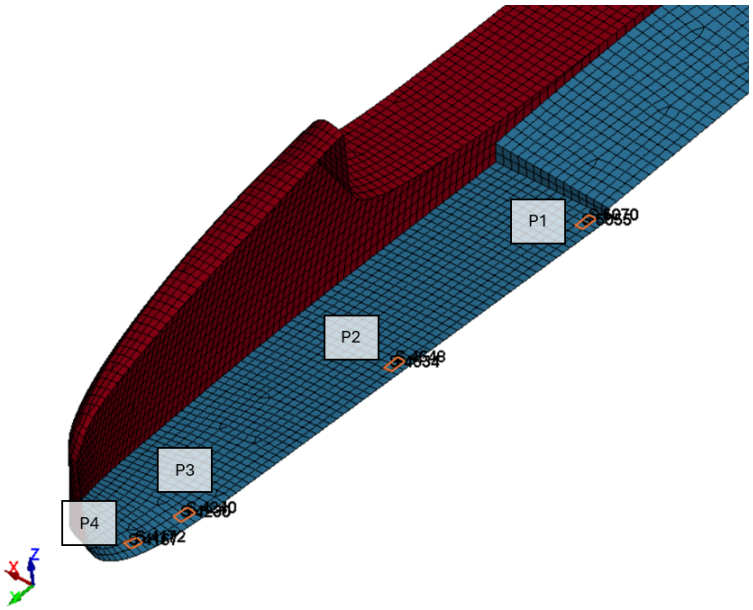

Figure 21 – Sensors' position on the hull

The sensors were positioned near the keel of the hull, mirroring their placement on the wedge to ensure consistent data collection. They were installed at points on the hull where the dihedral angles corresponded to those used in previous wedge analyses.

3.1 Analysis considering only vertical velocity

In the initial phase of the hull analyses, only vertical velocity was implemented. The obtained results show the behavior of the first three sensors, as the fourth sensor, positioned at the dihedral angle of 20°, exhibits significantly lower pressure values.

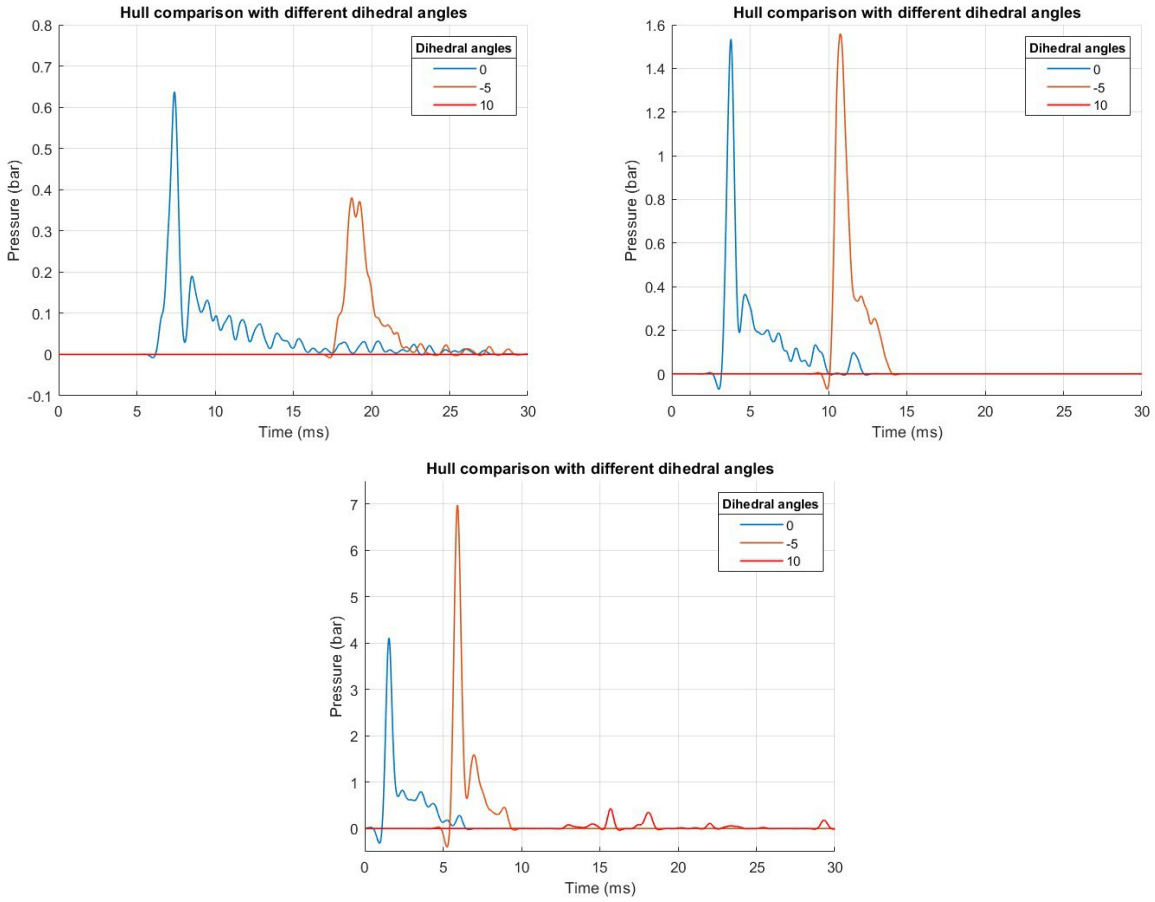

Figure 22 – Comparison of pressure varying dihedral angle at 1m/s, 2 m/s and 5m/s

Figure 22 sequentially illustrates the pressures on the hull at three different dihedral angles for analyses conducted at velocities of 1 m/s (top-left), 2 m/s (top-right), and 5 m/s (bottom). The pressures in the regions at 0° and -5° exhibit a trend where the maximum pressure appears at low velocities near the 0-degree region, while at higher velocities, it shifts to the negative dihedral angle region. This phenomenon is attributed to the elasticity of the structure; at low velocities, the behavior can be likened to that of a rigid body, whereas at higher velocities, the structure at 0° can undergo greater deformation, thereby dissipating the pressure exerted on it.
Regarding the absence of pressure at 1 m/s and 2 m/s in the 10-degree region, this is due to the duration of the simulation, as that portion remains dry. However, as seen in the 5 m/s case, the pressure on that sensor is still an order of magnitude lower compared to the other two regions due to the deceleration following the impact. Therefore, further analyses were not conducted, as the pressure in this region is not critical for dimensioning purposes.

3.2 Comparison with the wedge

This paragraph compares the pressures obtained on the wedge at 0° at sensor P1, in the absence of air in the model, with those on the hull where the dihedral angle is zero, also denoted as P1. A two-dimensional analysis would typically predict higher pressures due to the absence of edge and three-dimensional effects, which would otherwise result in lower pressures. However, in our case, this is not observed due to the geometric complexity of the hull and the manner of its impact. It is insufficient to consider a section of the hull as equivalent to a wedge since the dihedral angle varies and a sufficiently wide area comparable to the wedge cannot be identified. Additionally, in a two-dimensional case, water impacts the wedge simultaneously along every section of the y-axis, which does not occur with the hull. Initially, water impacts only a small section of the hull and then gradually spreads over a larger area. The hull's mass of 6.4 kg causes it to decelerate more slowly compared to the wedge, which has a mass of 0.126 kg. This is reflected in the rigid body accelerations of the

two models, where the wedge exhibits significantly higher values. However, when multiplied by their respective masses, the resulting force is lower for the wedge compared to the hull. The greater force on the hull results in higher pressures on the selected sensor for the hull, as shown in Figure 23.

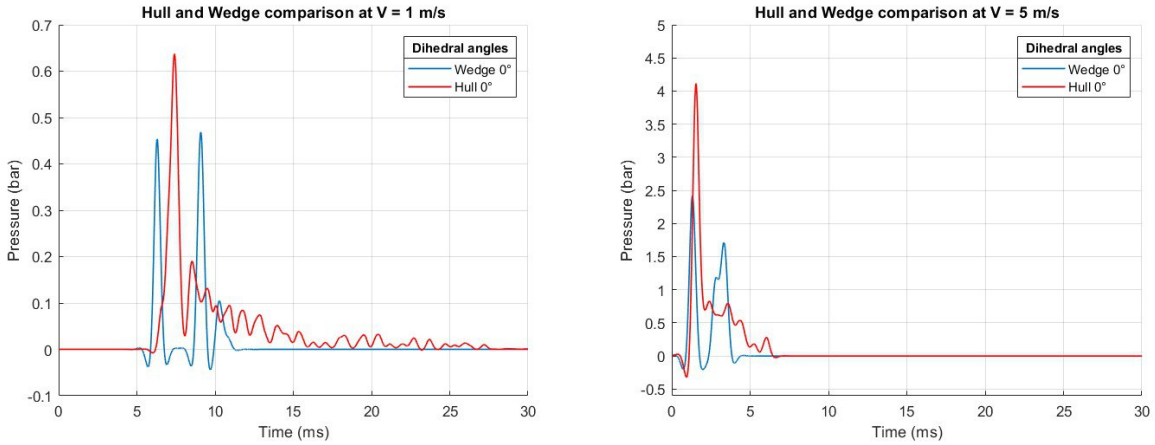

Figure 23 – Comparison between the wedge and the hull with the same dihedral angle

3.3 Analysis considering horizontal velocity

An additional analysis was performed on the hull to incorporate horizontal velocity, aiming to more accurately simulate the real-life conditions of a seaplane landing. For this scenario, the horizontal velocity was estimated to be about four times the vertical velocity. Consequently, the simulations were conducted with a vertical velocity of 1 m/s and a horizontal velocity of 4 m/s.

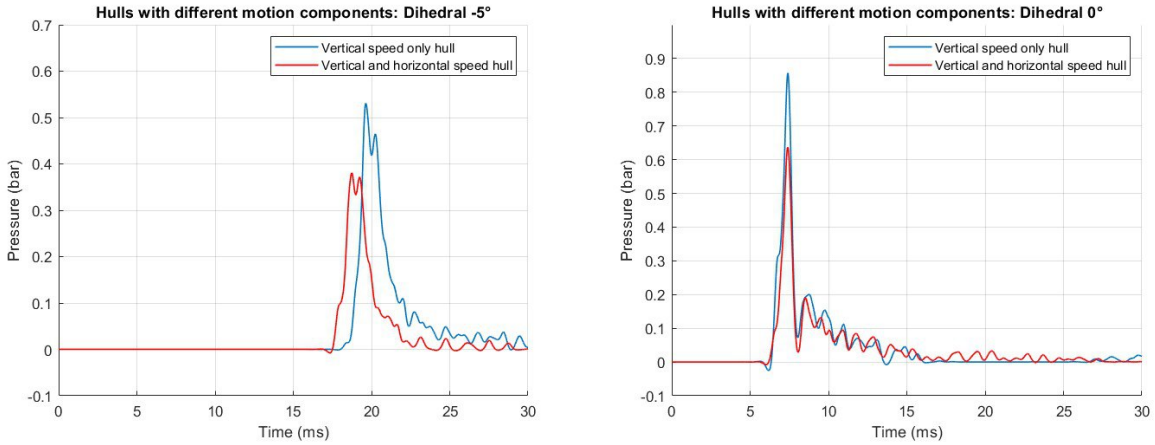

Figure 24 – Comparison between only vertical velocity and the addition of horizontal velocity

As shown in Figure 24, the pressure in the case with only vertical velocity is approximately 25% higher than in the case where horizontal velocity is also present. This phenomenon can be explained by the three-dimensional nature of the problem. During the fall with both vertical and horizontal velocities, the impact angle isn't perpendicular to the surface of water causing the forces to get distributed over a larger surface area in contact with the water, and the rotation around the x-axis causes a reduction in pressure by dissipating energy, leading to lower pressure values.

4. Future works

Future models will include the air surrounding the hull and the composite material used in the hulls, enhancing simulation and physical characterization, with the center of mass correctly positioned in the hull model. This will enable more accurate studies of rotations about the longitudinal, transverse,

and vertical axes during impact. Studying how different components of angular velocity influence pressures and forces will be crucial. Experimental validation is also essential to confirm the accuracy of numerical models and analytical theories used in the study. In addition, empirical results will facilitate the development or improvement of existing theories, leading to a deeper understanding of fluid-structure interactions and enhancing the design and safety of seaplanes and other water-interacting vehicles.

5. Conclusions

The study examined the impact of the hull of the S55 seaplane on a calm water surface, focusing on the portion of the hull that first makes contact with the water, between 50% and 90% of its total length, where the dihedral angle varies between -5 and 20 degrees. To achieve this, the study and analysis of simple two-dimensional models were initially conducted to determine the pressure values that develop on structures impacting at a certain velocity with a specific dihedral angle. The results were compared with those predicted by Von Karman [5] and Wagner's [6] theories, and it was found that as the impact velocity increases, the deformation of the elastic body, as considered in this study, tends to reduce the pressure. Additionally, the behavior of air was investigated, revealing a beneficial effect on the stresses developed in the structure. This effect is particularly noticeable at 0°, where the air pocket formed reduces the pressure by approximately 77%. Subsequently, the behavior of the hull and the effect of the three-dimensional nature of the problem were further investigated. Significant variations in pressure distribution on the hull's surface were observed when using a comprehensive model, which differs markedly from those in two-dimensional models employing wedges. The study also investigated how pressures vary with the addition of a longitudinal velocity component, aiming to evaluate in future scenarios the pressures that develop when the horizontal velocity significantly exceeds the vertical component.
In conclusion, to thoroughly understand the behavior of a structure during water impact, it is essential to consider various factors, primarily its shape and the section that impacts first. Finally, excluding air in a numerical model might be sufficient for confidently sizing a structure, but it results in significantly higher pressures, especially for flat structures or those with negative dihedral angles.

6. Acknowledgment

The authors express their gratitude to the Politecnico di Torino and the DIMEAS department for the provision of resources and facilities. We also extend our thanks to DAUIN for the computational resources provided through High Performance Computing Polito (HPC@POLITO), a project of Academic Computing within the Department of Control and Computer Engineering at the Politecnico di Torino (http://www.hpc.polito.it). Special thanks go to ANSYS and EnginSoft Italy for their support and for providing the software licenses.

7. Copyright Statement

References

[1] Cestino E, Frulla G, Sapienza V, Pinto P, Rizzi F, Zaramella F, Banfi D. "Replica 55 Project: A Wood Seaplane in The Era of Composite Materials". ICAS 2018 31st Congress of The International Council of the Aeronautical Sciences, Belo Horizonte, 2018.

[2] Valpiani F, Polla A, Cicolini P, Grilli G, Cestino E, Sapienza V. "Early Numerical Evaluation of Fluid-Structure Interaction of a Simply Wedge Geometry with Different Deadrise Angle." AIDAA XXVI International Congress, Pisa, 2021.

[3] F. Valpiani, P. Cicolini, D. Esposto, A. Galletti & D. Guagliardo. "Numerical modeling of Fluid-Structure Interaction of a 3D wedge during water impact with variation of velocity and pitch angle." 33rd ICAS Congress 4-9 September 2022 – Stockholm, Sweden.

[4] Guagliardo D., Cestino E., Nicolosi G., Guarino E., Virdis A., Alfero A., Pittalis D, Sabella M. "Impact of a wedge in water: assessment of the modeling keyword, presence of cavitation and choice of the filter most suitable for the case study" AIDAA XXVII International Congress, Padova, 2023.

[5] Von Kármán, Th. 1929. "The Impact on Seaplane Floats During Landing". National Advisory Committee on Aeronautics.

[6] Wagner H. Über Stoß- und Gleitvorgänge an der Oberfläche von Flüssigkeiten. "Zeitschrift Für Angewandte Mathematik Und Mechanik", Vol. 12, No. 4, 1932.

[7] S. Okada e Y. Sumi, "On the water impact and elastic response of a flat plate at small impact angles" Journal of Marine Science and Technology, 2000.

[8] Hughes, K. & Campbell, J. (2008). "Helicopter Crashworthiness: A Chronological Review of Research Related to Water Impact from 1982 to 2006". Journal of The American Helicopter Society - J AMER HELICOPTER SOC. 53. 10.4050/JAHS.53.429.